Bioresource Technology Reports 34 (2026) 102638

Contents lists available at ScienceDirect

Bioresource Technology Reports

journal homepage: www.sciencedirect.com/journal/bioresource-technology-reports

Integrated biorefinery scheme for apple pomace: Synergistic extraction and fermentation for dual recovery of pectin and 2,3-butanediol

Alberto Lozano, Alba Mei González-Galán, Juan Carlos López-Linares, Mónica Coca, María Teresa García-Cubero, Susana Lucas *

Department of Chemical Engineering and Environmental Technology, University of Valladolid, Dr. Mergelina s/n, 47011, Valladolid, Spain
Institute of Sustainable Processes, Department of Chemical Engineering and Environmental Technology, University of Valladolid, Dr. Mergelina s/n, 47011, Valladolid, Spain

ARTICLE INFO

Keywords:
Apple pomace
Microwave-Assisted Extraction
Ultrafiltration
Pectin
2,3-butanediol

ABSTRACT

This study presents an integrated, solvent-free biorefinery approach that couples microwave-assisted extraction (MAE), ultrafiltration (UF), and separate enzymatic hydrolysis and fermentation (SHF) to co-produce pectin-derived oligosaccharides (POS), predominantly oligogalacturonides (OGalA), and 2,3-butanediol (2,3-BDO) from apple pomace (AP). Through response surface methodology, optimized MAE temperature and time conditions to maximize OGalA formation were identified, while also limiting sugar degradation. Under these conditions (136 °C, 8.1 min), the extract contained OGalA at 4.0 ± 0.2 g/L, corresponding to a recovery of 53.7 ± 0.8%, and a pectin yield of 22.3 ± 0.2% was achieved (dry AP basis). Subsequently, an ultrafiltration step using a 3 kDa membrane yielded an OGalA solution concentrated to 11.5 ± 0.1 g/L and partially depleted small molecules. Compositional profiling also confirmed a notable enrichment of the rest of the oligosaccharide fractions, with increases ranging from 2.4- to 3.2-fold. In parallel, the MAE-pretreated solid, selectively depleted in pectic domains and enriched in glucan (~37%), was saccharified and fermented via a sequential hydrolysis-fermentation scheme to produce 2,3-BDO. Fermentation trials with *Bacillus* strains achieved concentrations of 10.3 ± 0.4 g/L (*B. amyloliquefaciens*) and 9.5 ± 0.2 g/L within 47 h (*B. licheniformis*), with sugar clearance below 48 h at 10–15% (*w/v*) solids loading. In conclusion, an integrated MAE → UF → SHF configuration co-producing POS and 2,3-BDO offers a practical route to valorize AP and advance circular bioeconomy goals in fruit-processing regions.

1. Introduction

Apple pomace (AP), a major by-product of the apple industry, is traditionally discarded, creating significant environmental concerns. However, it is now recognized as a globally abundant agro-industrial byproduct, with an annual production estimated at approximately 12 million tonnes (based on recent FAOSTAT-derived estimates for the 2020–2022 period). As a low-cost or even negative-cost feedstock due to disposal regulations, AP represents a valuable substrate for biotechnological applications. Unlike typical lignocellulosic biomass (LCB), which consists of a rigid and highly recalcitrant matrix with high lignin content (typically 20–30%) and negligible pectic fractions, AP is characterized by a significantly lower lignin concentration, ranging from 9.5% to 18.9% (Jasińska et al., 2024; Yilmaz-Turan et al., 2023). Furthermore, AP stands out due to its high pectin concentration, which can constitute 10–25% of its dry matter (Costa et al., 2025; Wang et al., 2025). This unique structural composition is advantageous, as it facilitates the use of milder processing conditions—such as the microwave-assisted extraction (MAE) optimized in this study—enabling the simultaneous recovery of functional pectic oligosaccharides and fermentable sugars. Its rich composition in complex carbohydrates and polyphenolic antioxidants (Fariñas-Mera et al., 2025) also makes it an ideal candidate for valorization into biofuels such as ethanol (Ma et al., 2024) and butanol (Bravo-Venegas et al., 2023). Ultimately, this approach transforms a waste stream into a high-value resource, aligning perfectly with circular economy principles (Białkowska et al., 2015; Kauser et al., 2024).

* Corresponding author at: Institute of Sustainable Processes, University of Valladolid, School of Industrial Engineering, Dr. Mergelina s/n, 47011, Valladolid, Spain.
E-mail addresses: alberto.lozano@uva.es (A. Lozano), albamei.gonzalez.galan@uva.es (A.M. González-Galán), juancarlos.lopez.linares@uva.es (J.C. López-Linares), monica.coca@uva.es (M. Coca), mtgarcia@uva.es (M.T. García-Cubero), susana.lucas.yague@uva.es (S. Lucas).

https://doi.org/10.1016/j.biteb.2026.102638
Received 24 November 2025; Received in revised form 9 February 2026; Accepted 11 February 2026
Available online 17 February 2026

Pectin, a key component of AP, is widely utilized in the food, pharmaceutical, and cosmetic industries due to its thickening, gelling, and health-promoting properties (Roman-Benn et al., 2023). In traditional industrial processes, commercial pectin is predominantly sourced from citrus peels and apple pomace (Wang et al., 2025). As the third-largest food hydrocolloid by revenue, the pectin market is projected to double from $1 billion in 2019 to $2 billion by 2026 (Jia et al., 2024). Additionally, the prebiotic potential of AP is attributed to its fermentable fibers and oligosaccharides, which support beneficial gut microbiota and functional food development (Maina et al., 2022).

Traditional pectin extraction involves acid treatment and ethanol precipitation, which is effective but energy-intensive and environmentally burdensome (Matharu et al., 2016). Sustainable alternatives such as MAE, Radio Frequency-Assisted Extraction (RFAE) (Zheng et al., 2021), Ultrasound-Assisted Extraction (UAE) (Girón-Hernández et al., 2023), and Subcritical Water Extraction (SWE) (Yilmaz-Turan et al., 2023) offer reduced energy use and processing time while enhancing yield. However, the large-scale adaptation of these technologies remains selective. In the case of UAE, processing high-solid apple pomace slurries—which are characterized by high viscosity and non-Newtonian behavior—is hindered by significant acoustic impedance. This causes rapid ultrasonic wave attenuation, effectively restricting the cavitation zone to the immediate vicinity of the transducers (Girón-Hernández et al., 2023; Zheng et al., 2021). Consequently, energy transfer efficiency is severely compromised in large-scale reactors, leading to non-uniform extraction and 'dead zones' where the biomass remains untreated. Furthermore, increasing power to overcome attenuation often results in localized overheating, which can degrade the pectic structure. Conversely, SWE involves high capital investment and stringent safety protocols for high-pressure operations (Yilmaz-Turan et al., 2023). In this context, MAE stands out as a more industrially mature and modularly scalable configuration, providing a balanced trade-off between technological intensification and operational feasibility for the valorization of food waste such as AP (Costa et al., 2025). By utilizing dielectric heating, MAE ensures volumetric energy delivery that is less dependent on the rheological properties of the slurry (Matharu et al., 2016; Zheng et al., 2021). In addition to its industrial scalability, MAE stands out for its efficiency. Operating under mild conditions (pH 2–3, 80–90 °C, 5–19 min), MAE has yielded up to ~10.6–10.9% pectin with a galacturonic acid content above 50–60% using citric acid as solvent (Costa et al., 2025; Zheng et al., 2021). This reinforces MAE's role in integrated biorefineries for recovering bioactives from AP.

Membrane-based separations complement green extraction methods. Ultrafiltration (UF) offers not only a solvent-free and scalable method to purify pectin-derived oligosaccharides (POS), but also the selective recovery of neutral sugars and low-molecular-weight oligosaccharides with recognized prebiotic potential. Unlike conventional ethanol precipitation—which requires large solvent volumes, partial neutralization steps, and may lead to the loss of soluble oligosaccharides—UF allows continuous operation, easy scalability, and better preservation of functional bioactives. Using ceramic membranes (100, 10, and 1 kDa), Ruiz et al. (2024) achieved up to 87% POS recovery from onion skin extracts, with effective removal of low-molecular-weight impurities while preserving their functionality.

Beyond their use as independent purification steps, UF has also been incorporated into broader membrane-based valorization schemes for fruit-processing by-products, enabling the concentration and fractionation of pectin-rich and other bioactive streams after thermo- or extraction-based solubilization. In this context, recent reviews on pectins recovered from food-waste streams emphasize that the coordinated design of extraction and membrane fractionation stages plays a critical role in determining both process sustainability and the techno-functional properties of the resulting pectin-derived products (Tsirigotis-Maniecka et al., 2024). However, most existing approaches remain limited to two-stage extraction–UF purification schemes, leaving scope for broader integration of upstream fractionation with downstream valorization routes in apple-pomace biorefineries.

The production of 2,3-butanediol (2,3-BDO)—a versatile platform chemical for multiple industries (Song et al., 2019)—represents another key valorization pathway for AP hydrolysates. Owing to its broad downstream conversion routes, 2,3-BDO serves as a precursor for high-value chemicals such as methyl ethyl ketone (a solvent used in coatings, lubricants, adhesives, fuels, and inks), as well as flavor and fragrance compounds including acetoin and diacetyl; moreover, its physicochemical properties support applications in cosmetics, skincare formulations, and antifreeze products (Gawal and Lataye, 2025; Gawal and Subudhi, 2023). This biotechnological production is typically achieved via fermentation with industrially relevant, non-pathogenic strains like *Bacillus licheniformis* and *Bacillus amyloliquefaciens* (Jurchescu et al., 2013). The potential of this approach is well-documented, with studies showing a progression from 16.5 g/L in batch systems to ~60 g/L using fed-batch methods (Sikora et al., 2016). These efforts have been extended to optimized and scaled fermentation conditions in both shake flasks and bioreactors, demonstrating the feasibility of integrating AP into efficient bio-based production systems (Białkowska et al., 2015; Sikora et al., 2016). Furthermore, recent technology-roadmapping analyses emphasize that the industrial viability of 2,3-BDO production depends on the joint optimization of upstream processing, fermentation operation, and downstream recovery steps, reinforcing the relevance of integrated biorefinery approaches (Tinôco et al., 2021a).

This study establishes a novel, integrated, and membrane-driven biorefinery model for AP that simultaneously targets the recovery of a functional pectin-rich fraction—comprising both oligogalacturonides (OGalA) and neutral oligosaccharides with prebiotic potential—alongside the platform chemical 2,3-BDO from a single feedstock. To achieve this, the investigation was structured around three interconnected goals: (1) optimizing MAE to maximize the release of OGalA while suppressing byproduct formation, (2) evaluating the performance of UF for the selective purification and concentration of the pectic extract, and (3) valorizing the residual MAE-derived solid fraction through enzymatic saccharification followed by microbial fermentation with *Bacillus licheniformis* and *Bacillus amyloliquefaciens*.

In contrast to conventional processes that rely on ethanol precipitation—where the recovery of neutral oligosaccharides is often incomplete and solvent consumption remains high (Ziadi et al., 2018)—this triple-process configuration demonstrates a scalable, membrane-based alternative that enhances both product yield and environmental performance. By integrating green extraction, membrane purification, and biotechnology, this dual-product strategy transforms industrial waste into a high-value bioproduct portfolio. This model advances circular economy principles and directly supports SDG 9 and SDG 12, reinforcing the critical role of integrated biorefinery frameworks in sustainable development.

2. Materials and methods

2.1. Raw material

The AP was kindly provided by the company Muns Agroindustrial (Lérida, Spain). This was a byproduct generated from pressing apples during apple juice production. The AP was oven-dried at 60 °C and then ground to a particle size of 1–3 mm in a household blender before the experiments.

2.2. Pectin recovery by microwave-assisted extraction

The scheme of the process for pectin recovery can be found in Fig. 1. MAE was conducted using a closed microwave-assisted reaction system (Multiwave PRO SOLV reactor 50 Hz with rotor type 16HF100, Anton Paar GmbH, Austria, Europe). A mixture of AP and distilled water was prepared in 100 mL PTFE-TFM vessels containing magnetic stirrers. The vessels were housed in ceramic pressure containers, one of which was

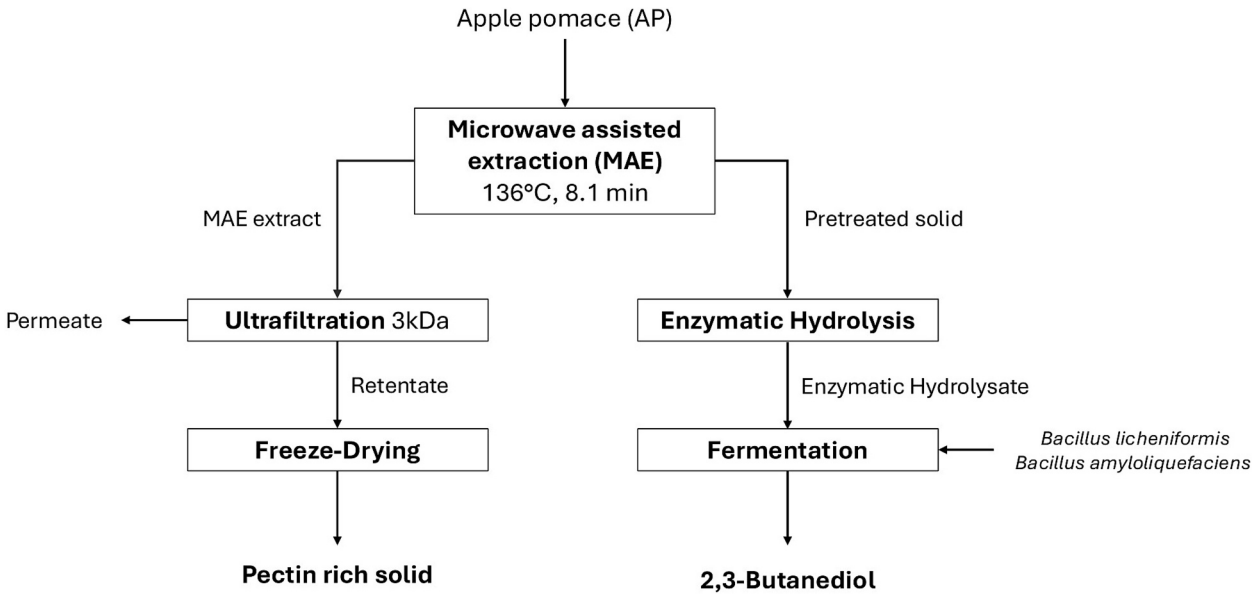

Fig. 1. Schematic diagram for obtaining the pectin and pectin-derived oligosaccharides products from aple pomace used in the study.

fitted with a combined pressure and internal temperature sensor. Temperature sensors monitored all vessels using an infrared (IR) detector, and the system dynamically regulated microwave energy based on pressure and temperature feedback. The solid-to-liquid ratio of the AP and water mixture was set at 10% (*w/v*), comprising 5 g of dried AP and 50 mL of distilled water. The heating rate was maintained at 6 °C/min to reach the target temperature. Following the extraction process, the pressure vessels were cooled to 55 °C. The solid and liquid fractions were subsequently separated by vacuum filtration. The solid fraction was dried at 45 °C for 48 h in a drying oven (Memmert, Schwabach, Germany) and weighed to calculate solid recovery (g of solid fraction after pretreatment/g of initial AP). The liquid fraction was stored at 4 °C for further HPLC analyses, including the quantification of monomeric sugars, oligomers, and degradation products.

2.3. Experimental design for pectin extraction

To optimize the extraction conditions for pectin via MAE, a response surface methodology based on a Central Composite design (RSM-CCD) was employed. The parameters selected were MAE temperature (X_1) and MAE time (X_2). The factorial region of the design covered 115–155 °C and 5–15 min, while axial points extended the experimental domain to 107–163 °C for temperature and 2.9–17.1 min for time (Table 1). The intervals of the variables were selected based on previous results (data not shown). In order to measure the harshness of the pretreatment, the Severity Factor (SF) was calculated according to previous studies (MacAskill et al., 2018) (Eq. (1)), where t is time (min) and T is temperature (°C).

$$Severity\ factor\ (SF) = Log\left[t{\cdot}exp\left(\frac{T-100}{14.75}\right)\right] \quad (1)$$

The response variable was the concentration of OGalA. A total of 11 experiments were planned using R (Table 1), including one central point tested in triplicate to estimate the experimental error and assess model reproducibility. Finally, three confirmatory experiments were performed under the optimized conditions predicted by the statistical model to validate the results.

2.4. Purification step by UF

The MAE extract obtained under optimal conditions underwent a purification process using membrane ultrafiltration, carried out in a Minimate tangential filtration system (Pall Corporation, USA) equipped with a polyethersulfone membrane with a Molecular Weight Cut-Off (MWCO) of 3 kDa and a filtration area of 50 cm^2. Prior to UF, the extract underwent centrifugation (Thermo Scientific, Sorvall X Pro Series, Waltham, MA, USA) followed by vacuum filtration, through 0.45 and 0.22 μm membranes to eliminate larger particles.

The ultrafiltration process was conducted at room temperature, maintaining a constant transmembrane pressure (TMP) of 1.38 bar. The feed solution was continuously stirred with a magnetic stirrer to maintain homogeneity and minimize concentration polarization at the

Table 1
Response Surface Methodology – Central Composite Design (RSM-CCD) conditions for pectin extraction by MAE. Extract pH, solid recovery and Severity Factor (SF).

Run	Independent variables				Extract pH	Solid recovery (%)	SF
	x_1	X_1 (Temperature, °C)	x_2	X_2 (Time, min)			
1	+α	163	0	10	3.5 ± 0.1^a	37.9 ± 1.0^a	2.9
2	0	135	0	10	3.5 ± 0.0^a	48.2 ± 0.3^b	2.0
3	+1	155	+1	15	3.6 ± 0.1^b	39.2 ± 0.4^a	2.8
4	0	135	0	10	3.5 ± 0.0^a	49.7 ± 0.3^b	2.0
5	0	135	-α	2.9	3.4 ± 0.0^a	51.3 ± 3.2^c	1.5
6	-1	115	-1	5	3.5 ± 0.1^a	46.0 ± 0.8^b	1.1
7	0	135	0	10	3.5 ± 0.0^a	43.1 ± 1.3^a	2.0
8	+1	155	-1	5	3.6 ± 0.0^b	52.8 ± 2.9^c	2.3
9	-α	107	0	10	3.4 ± 0.0^a	49.8 ± 0.2^b	1.2
10	-1	115	+1	15	3.6 ± 0.0^b	45.4 ± 0.1^b	1.6
11	0	135	+α	17.1	3.6 ± 0.0^b	40.7 ± 0.3^a	2.3

Different letters within a column indicate significant differences at $p < 0.05$ (Tukey's HSD).

membrane surface. To lower viscosity and facilitate the removal of small molecules and impurities, the extract (100 mL) was diluted with water, reaching a final volume of 300 mL before ultrafiltration. This dilution step was crucial to keep the pectic concentration below the critical gelation threshold, thereby ensuring efficient permeate flux and preventing the formation of a restrictive gel layer on the membrane—a common bottleneck when processing high-molecular-weight polysaccharides like pectin.

The process operated in concentration mode until the retentate volume was reduced to one-fourth of the initial feed volume (Concentration Factor = 4). To evaluate the efficiency of the separation, the recovery yield (Yi, %) of each component (monosaccharides, oligosaccharides, degradation compounds) in the retentate was calculated using Eq. (2):

$$Y_i = \frac{C_{R,i} \cdot V_R}{C_{0,i} \cdot V_0} \cdot 100 \quad (2)$$

where $C_{R,i}$ and $C_{0,i}$ represent the concentration (g/L) of component i in the final retentate and the initial feed (diluted extract), respectively, while V_R and V_0 correspond to their respective volumes (L).

Additionally, the Enrichment Factor (EF) was determined to quantify the concentration efficiency of the membrane for specific target compounds, calculated as the ratio between the final concentration in the retentate ($C_{R,i}$) and the initial concentration in the feed ($C_{0,i}$), according to Eq. (3):

$$EF = \frac{C_{R,i}}{C_{0,i}} \quad (3)$$

Further details regarding the UF protocols and operational parameters are available in our previous work (del Amo-Mateos et al., 2024).

2.5. Model for membrane fouling

Hermia models were proposed to describe the flux decline in the tangential-flow UF process. At the beginning of the UF process, the flux depends on membrane resistance and decreases over time due to membrane fouling. These mechanisms include pore blocking and cake formation. The linear models for these cases are given by the following equations (Lim and Bai, 2003): membrane resistance-limited (Eq. (4)), pore blocking resistance-limited (Eq. (5)) and cake resistance-limited (Eq. (6)).

$$\frac{1}{J} = \frac{1}{J_0} + K_m \cdot t \quad (4)$$

$$\ln(J) = \ln(J_0) + K_P \cdot t \quad (5)$$

$$\frac{1}{J^2} = \frac{1}{J_0^2} + K_C \cdot t \quad (6)$$

where J is the permeate flux ($m^3/(m^2 \cdot s)$), J_0 is the initial permeate flux ($m^3/(m^2 \cdot s)$), K_m, K_P and K_C are the membrane, pore blocking and cake constants, respectively, and t is the time (s). After fitting the experimental data to the models, J_0 was calculated as the average of the J_0 fit parameter of each model.

2.6. Production of 2,3-Butanediol from pretreated AP

Microorganisms used in this study were *Bacillus licheniformis* and *Bacillus amyloliquefaciens*, both from the German microorganism collection (DSMZ, Leibniz, Germany), which were stored as glycerol stock (40% (*v*/v)) at −80 °C. Both inocula were grown in 250 mL Erlenmeyer flasks (at 37 °C and 150 rpm for 24 h, in a rotary shaker, Optic Ivymen System, Comecta, Spain), using 50 mL of basal medium as described by Jurchescu et al. (2013). The basal medium contained (per liter): 20 g glucose, 5 g yeast extract, 5 g Bacto tryptone, 7 g K_2HPO_4, 5.5 g KH_2PO_4, 1 g $(NH_4)_2SO_4$, 0.25 g $MgSO_4 \cdot 7H_2O$, 0.12 g $Na_2MoO_4 \cdot 2H_2O$, 0.021 g $CaCl_2 \cdot 2H_2O$, 0.029 g $Co(NO_3)_2 \cdot 6H_2O$, 0.039 g Fe $(NH_4)_2(SO_4)_2 \cdot 6H_2O$, and 10 mL trace elements. The trace elements solution contained (per liter): 0.2 g nicotinic acid, 0.0262 g $Na_2SeO_3 \cdot 5H_2O$, 0.0037 g $NiCl_2 \cdot 6H_2O$, 0.5 g $MnCl_2 \cdot 4H_2O$, 0.1 g H_3BO_3, 0.0172 g $AlK(SO_4)_2 \cdot 12H_2O$, 0.001 g $CuCl_2 \cdot 2H_2O$, and 0.554 g $Na_2EDTA \cdot 2H_2O$. All medium components were autoclaved (121 °C, 15 min), except the solutions containing $Co(NO_3)_2$ and $Fe(NH_4)_2(SO_4)_2$ as well as the trace elements solution, which were sterilized by filtration (using 0.2 μm cellulose nitrate filters). The inoculation was performed employing 1 mL of *B. licheniformis* or *B. amyloliquefaciens* glycerol stocks.

Regarding the 2,3-BDO fermentation process, firstly, the pretreated AP was enzymatically hydrolyzed at 10% *w/v* (25 g solid and 250 mL enzymatic solution) and 15% w/v (37.5 g solid and 250 mL enzymatic solution) substrate loading, employing 1000 mL Erlenmeyer flasks. Enzymatic hydrolysis was carried out, at least in duplicate, in an orbital shaker (Optic Ivymen System, Comecta, Spain), at 50 °C, 150 rpm, and pH 4.8 (adjusted with 10 M NaOH solution, without using any buffer to avoid possible interference in the subsequent fermentation stage) for 24 h. A mixture of Cellic CTec2 and Viscozyme L enzymes (both with an enzyme load of 10 FPU/g substrate), kindly donated by Novozymes A/S (Bagsvaerd, Denmark), was used. These conditions were chosen based on previous results (López-Linares et al., 2025a). The resulting enzymatic hydrolysates (separated from residual solids by vacuum filtration) were analysed for their sugar content, pasteurized (at 90 °C for 15 min), the pH was adjusted to 6.5 (using NaOH 10 M solution) and they were employed as fermentation broths for 2,3-BDO production.

2,3-BDO fermentation was conducted at 37 °C, 150 rpm, 144 h, and pH 6.5 (without control through fermentation), using 250 mL Erlenmeyer flasks and 50 mL of fermentation broth by flask. The same nutrients as those described in the pre-culture medium were used to supplement the enzymatic hydrolysates. Both *Bacillus* strains were inoculated at 4% (*v*/v). Samples were withdrawn during fermentation, centrifuged (at 13,500 x*g* for 10 min), and analysed for their contents in sugars, 2,3-BDO, ethanol, acetoin, and cells. Fermentation tests were carried out at least in duplicate.

2.7. Analytical methods

2.7.1. Biomass characterization

The pretreated-AP was characterized for its structural carbohydrates, lignin and ash content following the methods of the Laboratory Analytical Procedures of the National Renewable Energy Laboratory (NREL) (Sluiter et al., 2008a, 2008b) The extractive content of the AP was also determined according to the NREL methods, NREL/TP-510-42,619 (Sluiter et al., 2008c).

2.7.2. Analysis of sugar composition, galacturonic acid, fermentation products, and degradation compounds

To analyze the sugar composition (glucose, galactose, rhamnose, and arabinose), galacturonic acid (GalA) and degradation compounds (acetic and formic acids, 5-hydroxymethyl-furfural (HMF) and furfural) of both the optimal MAE extract and the retentate UF extract, High-Performance Liquid Chromatography (HPLC) with an Aminex column HPX-87H at 60 °C was used. Detection was performed with a refractive index detector (Waters 2414, USA). The operational conditions were 0.01 N H_2SO_4 as the mobile phase, at a flow rate of 0.6 mL/min, and an injection volume of 20 μL. Samples were injected without prior dilution in Milli-Q water.

In order to determine the oligomeric sugars in the extracts, an acid hydrolysis step (120 °C, 3% *w/v* H_2SO_4, 30 min) was carried out. Oligomeric compounds were calculated as the difference between the total free sugars or GalA after and before acid hydrolysis. Fermentation products (2,3-BDO, acetoin, ethanol, acetic and butyric acids, among others) were also determined by HPLC with the equipment described above. All samples were passed through 0.22 μm nylon filters before

being analysed. On the other hand, in order to study the cell concentration in 2,3-BDO fermentation samples, their optical density (OD) at 600 nm were determined employing a spectrophotometer (Uvmini−1240, Shimazu Suzhou Wfg., Kyoto, Japan).

2.8. Statistical analysis

All statistical analysis of the experimental data were performed using RStudio platform (version 2025.05.0 + 496) with R (version 4.5.0).

The significance of the terms was assessed using ANOVA, and the F-statistics and *p*-values were used to determine the most influential factors. In addition, statistical differences between fermentation conditions were evaluated using Student's *t*-test ($p < 0.05$).

3. Results and discussion

3.1. Characterization of AP

The compositional analysis of the raw AP (see Supplementary Material, Table S1) showed a high content of structural carbohydrates, accounting for nearly 50% of its dry matter. Glucan (28.7 ± 0.9%) and galactan (11.2 ± 0.3%) were the predominant polysaccharides, followed by galacturonan (7.0 ± 0.4%), rhamnan (2.7 ± 0.1%), and arabinan (2.6 ± 0.1%). This profile is in partial agreement with previous reports, where glucan and galacturonan also appeared as major components of AP (Yilmaz-Turan et al., 2023). The relatively low abundance of arabinan and rhamnan is consistent with prior compositional data on apple pomace, where the combined content of arabinose and rhamnose was reported to be approximately 7.9% (Viegas et al., 2024). However, the predominance of galactan over galacturonan deviates from the typical composition of commercial pectin sources such as citrus peel or sugar beet, where homogalacturonan is the dominant domain. This distinctive feature aligns with recent evidence highlighting the presence of highly branched rhamnogalacturonan-I (RG-I) regions in AP-derived pectin, particularly when extracted under mild or subcritical conditions (Girón-Hernández et al., 2023; Yilmaz-Turan et al., 2023).

The total lignin content was 12.7%, comprising 11.6 ± 0.8% acid-insoluble lignin and 1.1 ± 0.0% acid-soluble lignin. These values fall within the range shown in previous works for apple pomace, with the literature indicating total lignin content between 9.5% and 18.9%, depending on the apple variety and processing method (Jasińska et al., 2024). Additional components included ethanol extractives (9.6 ± 0.1%), water extractives (7.1 ± 0.4%), and ash (0.6 ± 0.0%). Water extractives were composed primarily of galactose (3.0 ± 0.2%), glucose (1.4 ± 0.0%), galacturonic acid (0.5 ± 0.0%), arabinose (0.5 ± 0.0%), and rhamnose (0.6 ± 0.1%). The ash content was low, consistent with values previously reported for AP (typically <1%) (Yilmaz-Turan et al., 2023).

3.2. Pectin extraction from AP by hydrothermal MAE

The effects of the MAE temperature and extraction time on pectin recovery from AP (Table 1) were assessed using a response surface methodology with a central composite design (RSM-CCD). To evaluate the reproducibility of the process and estimate the experimental error, three replicates were performed at the central point (temperature: 135 °C; time: 10 min). Additionally, two axial ("star") points at ±α (1.41) levels were included to account for potential curvature in the response surface.

The pH values of the extracts and the corresponding solid recovery percentages are presented in Table 1. As observed, the extract pH ranged from 3.4 (Runs 5 and 9) to 3.6 (Runs 3, 8, 10, and 11), with no significant influence from the independent variables. In contrast, solid recovery varied between 37.9% (Run 1) and 52.8% (Run 8), representing a 39.3% difference in the retained solid fraction, which reflects the substantial impact of MAE severity on biomass solubilization between the harshest and mildest conditions. The highest recovery values were associated with shorter extraction times (Runs 5 and 8), while the lowest recovery occurred in the run conducted at 163 °C (Run 1). The observed decrease in solid recovery is directly influenced by the severity of pretreatment, since such factors as temperature and time promote the solubilization of the non-structural and labile fractions (i.e., extractives and hemicellulose). These results align with previous findings on the importance of optimizing temperature and extraction time.

Fig. 2 presents the composition of the extracts obtained through MAE, detailing the concentrations of monomers, oligomers (OS), and degradation products. The monomer concentration (Fig. 2A) shows a relatively stable profile across the different runs, with a predominant presence of galactose (Gal) and lower levels of other sugars such as galacturonic acid (GalA), glucose (Glc), rhamnose (Rha), and arabinose (Ara). Notably, Experiment 5 (135 °C, 2.9 min) had the lowest monomer concentration, consistent with its short extraction time, which likely limited polysaccharide solubilization. A similar time-dependent effect has been observed in other MAE studies, where insufficient treatment time results in lower extraction efficiency compared with longer exposures (Spinei and Oroian, 2022). Taken together, these observations support the fact that milder MAE conditions may yield a lower monosaccharide release (Białkowska et al., 2015).

In contrast, the oligomer concentration (Fig. 2B) varies more significantly across the runs, with higher levels of AraOs and GlcOs observed in the initial runs, suggesting a more extensive hydrolysis of polysaccharides under these conditions. The presence of OGalA remains notable, reflecting the partial depolymerization of pectin-like structures. Although the main target of this work was the recovery of OGalA, which constitutes a major class of POS, the oligomeric profile of the extracts highlights the concomitant presence of neutral POS such as AraOS and GlcOS. Far from being undesired by-products, these fractions are of considerable interest due to their reported prebiotic, antioxidant, and immunomodulatory properties. Thus, the integrated recovery of both OGalA and neutral POS broadens the potential applications of the extracts, strengthening the role of apple pomace as a versatile feedstock in biorefinery schemes.

Degradation products (Fig. 2C) exhibit a distinct profile, primarily composed of acetic acid, formic acid, HMF, and furfural. These compounds tend to accumulate more in the Runs 1 and 3; while Run 9 shows the lowest concentrations, indicating that harsher extraction conditions promote the formation of these degradation products. This is particularly evident in Run 1 (163 °C, 10 min), which exhibits the highest concentrations of these products. Notably, HMF concentrations were consistently higher than furfural. This is consistent with the compositional profile of AP, which is richer in hexoses (glucan, galactan) than pentose-based polysaccharides, thereby favoring HMF-forming degradation pathways over furfural formation.

The severity factor (SF) values across the experimental runs ranged from 1.1 to 2.9 (Table 1), directly influencing the partition between extraction efficiency and byproduct formation. The most severe conditions (Run 1: SF = 2.9, 163 °C, 10 min) resulted in the lowest solid recovery (37.9%) and the highest concentration of degradation products (5.2 ± 0.3 g/L, Fig. 2C), symptomatic of extensive polysaccharide decomposition. Conversely, lower severity treatments, such as Run 6 (SF = 1.1, 115 °C, 5 min), prioritized solid preservation with minimal degradation, though yields of soluble oligomers were concomitantly lower. Correlation analysis identified a strong positive relationship ($R = 0.93$) between the SF and the total concentration of degradation products (C_{deg}, representing the sum of formic acid, acetic acid, HMF, and furfural). This dependence is quantified by the linear regression model $C_{deg} = 0.78\ SF + 2.71$; $R^2 = 0.86$), which predicts an average increase of 0.78 g/L in degradation byproducts for every unit increase in the severity factor within the investigated experimental range. These results are in line with the findings observed for each group of components separately, reinforcing the role of SF as a useful integrated indicator to interpret the balance between extraction efficiency and thermal

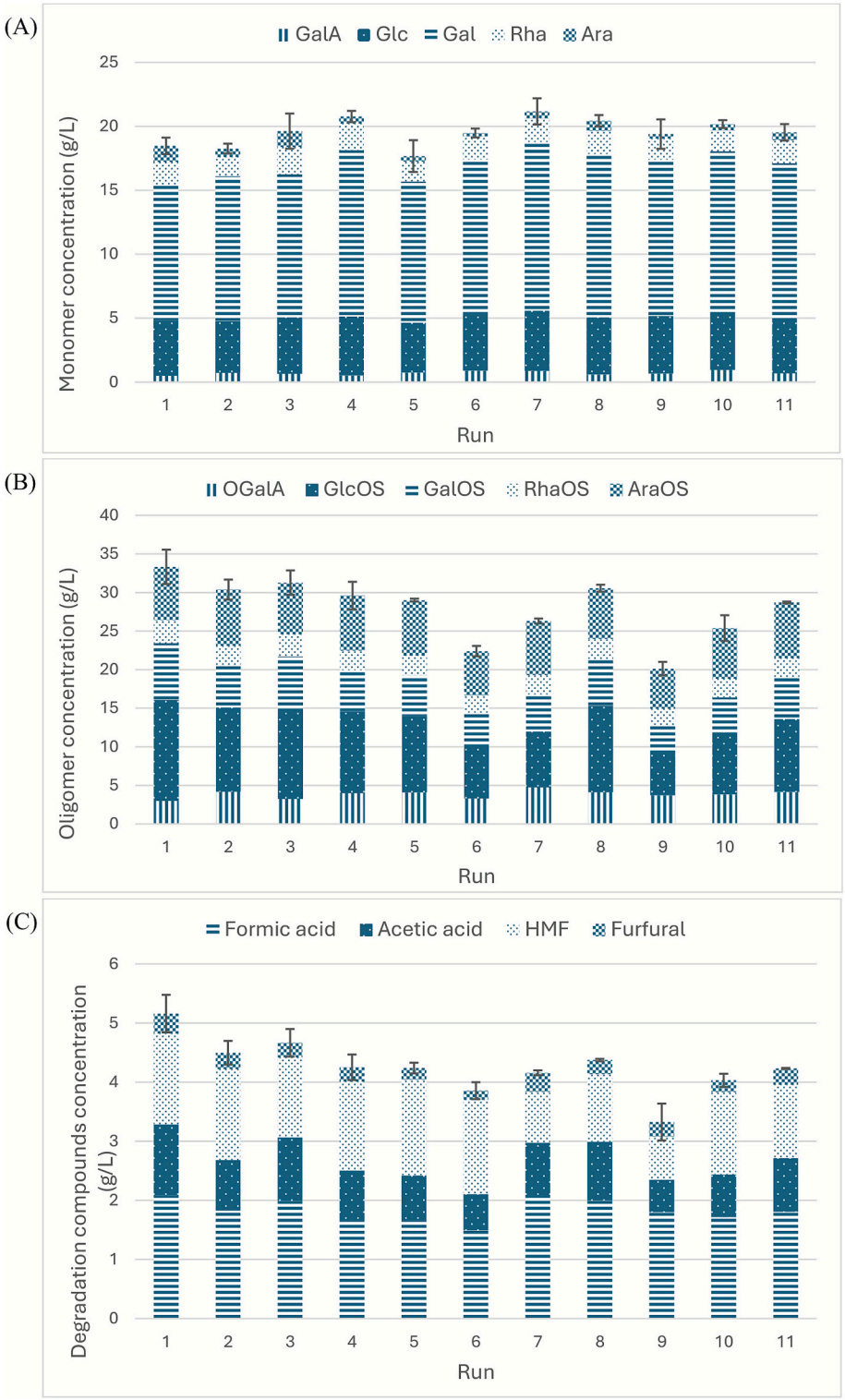

Fig. 2. RSM-CCD results: composition of the extracts. Monomer (A), oligomer (B), and degradation compound (C) concentrations.
GalA: galacturonic acid; Glc: glucose; Gal: galactose; Rha: rhamnose; Ara: arabinose; OgalA: oligogalacturonides; GlcOS: glucooligosaccharides; GalOS: galactooligosaccharides; RhaOS: rhamnooligosaccharides; AraOS: arabinooligosaccharides; HMF: 5-hydroxymethylfurfural.

degradation in microwave-assisted processes.

3.3. Optimization of OGalA extraction

3.3.1. Experimental design and model fitting

To identify the optimal MAE conditions for pectin recovery, the experimental data from the RSM-CCD were analysed using the rsm and stats packages of R software. A second-order polynomial model was fitted by least squares regression. ANOVA confirmed the adequacy of the model ($p < 0.05$) and revealed a significant curvature in the response surface, indicating that the system exhibits non-linear behavior and that a quadratic model is required to correctly describe the effect of

temperature and time on the response. Analysis of variance revealed that the linear effects were not significant as a group. Instead, a significant interaction between both variables and a pronounced quadratic effect of temperature were observed, demonstrating that OGalA recovery is governed by coupled and non-linear effects rather than monotonic trends. The lack-of-fit test was not significant (p-value = 0,179), confirming that the model adequately represents the experimental data within the studied domain (see Supplementary Material, Table S2). Moreover, the value of adjusted $R^2 = 0.9541$ showed that the model accounted for 95.41% of the variability in the recovery. The adequacy of the regression model was further supported by diagnostic plots of residuals, which showed normality, constant variance and the absence of systematic patterns (Supplementary Material, Fig. S1). Overall, these results validate the use of a quadratic response surface model to describe and optimize the MAE process.

The adjusted regression Eq. (7), predicting OGalA concentration as a function of temperature (T, in °C) and time (t, in minutes) demonstrated that both variables had quadratic effects on the response, with a significant interaction between them.

$$[OGalA] = -21.021 + 0.33147 \cdot T + 0.70359 \cdot t - 0.0035787 \cdot T \cdot t - 0.0011128 \cdot T^2 - 0.013442 \cdot t^2 \quad (7)$$

Further insight into the effect of individual variables was obtained from the regression analysis. Both temperature and time exhibited statistically significant linear effects ($p < 0.05$), with time showing a greater influence on pectin yield, as indicated by its higher coefficient value. Both linear terms showed a positive linear influence, meaning that increasing temperature or time individually tended to increase the amount of OGalA, up to a certain point.

In contrast, the quadratic terms for temperature and time were negative, indicating that excessive levels of either variable reduce extraction efficiency—likely due to thermal degradation. The interaction term between temperature and time was also significantly negative, though its effect was smaller in magnitude compared to the linear terms.

A response surface plot (see Supplementary Material, Fig. S2) was generated to visualize the influence of temperature and time on the OGalA concentration (g/L). The maximum OGalA concentration was achieved at intermediate temperatures and moderate extraction times, suggesting that both excessively high or low temperatures and/or times can negatively affect extraction efficiency due to degradation or insufficient solubilization. This is consistent with prior work showing that harsh thermal conditions during extraction can accelerate the breakdown of pectic chains and reduce final yield (Costa et al., 2025).

The optimization function within the rsm package was then used to predict the extraction conditions that maximize OGalA recovery. The optimal conditions were identified as 136 °C and 8.1 min, under which the model estimated a maximum OGalA concentration of 4.35 g/L.

3.3.2. *Characterization of the liquid extract under optimal MAE conditions*

Under the optimized MAE conditions, the liquid extract was characterized to determine its composition. This analysis was essential for evaluating both the selectivity of the extraction and the potential functional value of the resulting mixture.

The primary oligosaccharide fractions identified in the liquid phase included OGalA, glucooligosaccharides (GlcOS), rhamnooligosaccharides (RhaOS), and arabino-oligosaccharides (AraOS) (Table 2). Among them, OGalA reached 4.0 ± 0.2 g/L, representing 53.7 ± 0.8% recovery relative to the content in raw AP; while the total pool of oligosaccharides accounted for 47.0 ± 0.2% recovery with respect to the initial material.

Although the concentration of free galactose monomers was relatively high (12 g/L), no detectable galactooligosaccharides (GalOS) were observed in the extract. This absence could be attributed to the relative susceptibility of galactose-containing side chains to hydrolytic cleavage under microwave-assisted and thermally stressed conditions. Heat and acidic environments are known to promote the degradation of oligosaccharides through cleavage of labile glycosidic linkages, leading to depolymerization and conversion into monosaccharides (Huang et al., 2022). In addition, measurable degradation losses of galactooligosaccharides during high-heat processing have been reported in real food matrices, further supporting the vulnerability of galactose-containing oligomers to thermally induced breakdown (Cais-Sokolińska et al., 2022). Therefore, any galactooligosaccharides initially formed were likely rapidly hydrolyzed into monomers under the combined effects of localized microwave heating, acidic pH, and water activity. Similar degradation pathways for galactose-containing residues and pectin side chains under thermal stress have been previously reported (Matharu et al., 2016).

Notably, the experimentally obtained OGalA concentration showed a minor deviation of only 8.0% from the predicted value (4.0 vs. 4.4 g/L), validating the high predictive accuracy of the response surface model (adjusted $R^2 = 0.9541$).

In addition to oligosaccharides, the presence of thermal degradation products was also evaluated. The combined concentration of compounds such as furfural, HMF, and organic acids was measured at 3.6 ± 0.2 g/L. Although microwave-assisted extraction involves the application of elevated temperatures, the relatively moderate accumulation of these degradation markers suggests that the selected extraction conditions were sufficiently mild as to preserve the structural integrity of the target oligosaccharides, consistent with previous studies reporting greater sugar degradation and higher furfural and HMF formation under more severe treatments, while low-severity conditions lead to minimal structural alteration (Batista et al., 2019).

These results demonstrate that the optimized MAE conditions balance extraction efficiency with thermal stability, selectively recovering POS while minimizing sugar degradation. The composition of the extract positions it as a promising raw material for valorization in the development of health-promoting food ingredients or bio-based functional

Table 2
Composition of the extract obtained under optimal MAE conditions and final retentate after 3 kDa Ultrafiltration (UF): pH, bioactive compounds, enrichment factors (EF), and recovery yields.

	Concentration (g/L)		Enrichment factor	Recovery yield (%)
	Extract	UF	UF	UF
Extract pH	3.4 ± 0.0	–	–	
Monomers	16.8 ± 0.0	16.6 ± 0.0	0.99 ± 0.01	
OGalA[a]	4.0 ± 0.2	11.5 ± 0.1	2.88 ± 0.15	71.8 ± 0.1
GlcOS[b]	6.4 ± 0.1	17.0 ± 0.1	2.66 ± 0.04	66.4 ± 0.1
GalOS[c]	0.0 ± 0.0	0.0 ± 0.0	–	–
RhaOS[d]	1.1 ± 0.0	3.5 ± 0.1	3.18 ± 0.09	79.5 ± 0.1
AraOS[e]	6.5 ± 0.1	15.5 ± 0.1	2.38 ± 0.04	59.6 ± 0.0
POS[f]	19.3 ± 0.1	47.5 ± 0.1	2.46 ± 0.01	61.5 ± 0.1
Degradation compounds[g]	3.6 ± 0.2	3.3 ± 0.0	0.92 ± 0.05	

[a] OGalA: Oligogalacturonoides.
[b] GlcOS: glucooligosaccharides.
[c] GalOS: galactooligosaccharides.
[d] RhaOS: rhamnooligosaccharides.
[e] AraOS: arabinooligosaccharides.
[f] OS: pectin-derived oligosaccharides.
[g] Degradation compounds: formic acid, acetic acid, 5-Hydroxymethylfurfural (HMF) and furfural.

additives.

3.4. POS purification and concentration

The purification and concentration of POS from the hydrolysate were conducted using an ultrafiltration membrane with MWCO of 3 kDa. The evolution of the permeate flux (J) over time is presented in Supplementary Material, Fig. S3. The permeate flux progressively declined throughout the filtration process, indicating gradual membrane fouling. Experimental data were fitted to a logarithmic decay model, expressed by Eq. (8).

$$J(t) = -1{\cdot}10^{-7} ln(t) + 3{\cdot}10^{-6} \quad (8)$$

with a coefficient of determination $R^2 = 0.9727$, confirming a strong correlation and supporting the presence of time-dependent fouling effects. The fitted kinetic constants and the initial flux derived from this model are summarized in Supplementary Material, Fig. S4.

To further investigate fouling mechanisms, classical Hermia models were applied. The complete pore blocking model (1/J vs. time) and intermediate blocking model (ln(J) vs. time) showed strong agreement with experimental data ($R^2 \geq 0.90$), see Supplementary Data, Fig. S4A and S4B. These results suggest that early-stage fouling is dominated by internal pore obstruction, which can be directly linked to the physicochemical profile of the MAE extract. The high-molecular-weight pectic fragments, specifically the highly branched RG-I domains identified in Section 3.5, possess a hydrodynamic volume significantly larger than the 3 kDa MWCO of the polyethersulfone membrane. This size disparity leads to the complete pore blocking mechanism, where bulky pectic chains act as rigid obstacles at the pore entrances. The subsequent fit of the intermediate blocking model reflects the behavior of the flexible neutral side chains (arabinans and galactans). Despite the initial dilution to 300 mL, a step taken to maintain the solution viscosity below the gelation threshold and ensure permeate flux, the cumulative concentration of POS (19.3 g/L) facilitates molecular crowding and chain entanglement. This allows pectic solutes to not only settle on the membrane surface but also to bridge across previously obstructed areas, leading to the transition from individual pore sealing to a more continuous fouling layer. Additionally, the resistance-in-series model ($1/J^2$ vs. time) offered insight into the contribution of intrinsic resistance, pore fouling, and cake formation (see Supplementary Data, Fig. S4C). While detailed characterization (e.g., SEM) is vital for industrial scale-up, this kinetic baseline establishes the necessary groundwork for preliminary process design and future pilot-scale trials.

Following ultrafiltration, the retentate exhibited a significant enrichment in POS (Table 2), with a total concentration of 47.5 ± 0.1 g/L. Among the individual oligosaccharide fractions, GlcOS (17.0 ± 0.1 g/L) and AraOS (15.5 ± 0.1 g/L) were the most abundant, followed by OGalA (11.5 ± 0.1 g/L) and RhaOS (3.5 ± 0.1 g/L). No GalOS was detected. In contrast, monomeric sugars were retained to a lesser extent (16.6 ± 0.0 g/L), while low-molecular-weight degradation compounds, such as acetic acid, HMF, and furfural were partially removed (3.3 ± 0.0 g/L in total). Compared to the original liquid extract prior to membrane filtration, the membrane process resulting in a notable enrichment of all oligosaccharide fractions, with enrichment factors ranging from 2.4-fold for AraOS up to 3.2-fold for RhaOS (Table 2). The concentration of degradation products remained nearly constant (3.3 ± 0.0 vs. 3.6 ± 0.2 g/L), indicating limited removal of these small molecules under the applied membrane conditions.

The quantitative performance of the membrane is summarized in Table 2 through the Enrichment Factors (EF). The high EF for RhaOS (3.18 ± 0.09) and OGalA (2.88 ± 0.15) compared to the EF of degradation compounds (0.92 ± 0.05) highlights the selective nature of the 3 kDa membrane.

These results highlight the effectiveness of the 3 kDa ultrafiltration membrane in concentrating oligosaccharides while maintaining a selective separation of low-molecular-weight compounds. Similar membrane-based processes have proven effective for refining POS mixtures from AP, sugar beet pulp, and other lignocellulosic residues (Antov et al., 2023; Ruiz et al., 2024). The comparative increase in oligosaccharide content supports the suitability of this membrane-based approach for refining POS-rich extracts obtained through microwave-assisted extraction.

3.5. Refined pectin characterization

The efficiency of the extraction process applied to AP was demonstrated by a solid pectin yield of 22.3 ± 0.2%, calculated as the ratio between the dry mass of recovered pectin —obtained after freeze-drying the liquid extract— and the initial dry weight of AP (g pectin/100 g dry AP). This pectin recovery is directly supported by the compositional changes observed in the pretreated solid (see Supplementary Material, Table S1). After MAE, galacturonan and rhamnan —the main structural components of homogalacturonan and rhamnogalacturonan I, respectively— were completely removed from the solid phase, while arabinan was almost fully depleted. These fractions are precisely those detected in the recovered pectin as OGalA and neutral oligosaccharides (RhaOS, AraOS and GalOS) (see Supplementary Material, Table S3), confirming that the microwave-assisted pretreatment selectively solubilized the pectic domains of the apple cell wall and transferred them to the liquid phase. In contrast, the relative enrichment of glucan in the residual solid reflects the preservation of the cellulose-rich fraction, which remains available for downstream fermentation. A systematic comparison of reported apple pomace pectin extraction yields and compositional features across different extraction technologies is provided in Table S4 (see Supplementary Material). This yield is substantially higher than those commonly reported for apple pomace pectins obtained by microwave-assisted or conventional acid extraction, which typically range between ~6 and 15% depending on the extraction conditions (Chen and Lahaye, 2021; Girón-Hernández et al., 2023; Zheng et al., 2021), and also exceeds or matches values reported for subcritical water extraction approaches (Yilmaz-Turan et al., 2023).

Detailed compositional analysis (see Supplementary Material, Table S3) provided significant insights into the structural characteristics of the isolated pectin. The high purity of the pectic material was confirmed by a cumulative content of POS of 71.5 ± 4.3%. This is consistent with similar studies, where POS products from fruit peels showed ~73.3% POS, and were interpreted as highly enriched pectic oligosaccharide fractions (Orrego et al., 2024). A key finding was the significant enrichment in oligosaccharides derived from neutral sugar sidechains, which are hallmarks of RG-I domains. Specifically, AraOS were the predominant component at 26.8 ± 1.0%, while GalOS accounted for 11.3 ± 1.0%. These values are markedly higher than those reported for apple pomace pectins obtained by microwave- or radio-frequency-assisted extraction, which are typically characterized by higher GalA contents and less pronounced neutral-sugar enrichment, indicative of more homogalacturonan-rich pectic structures with lower neutral sugar contents (Guo et al., 2024; Zheng et al., 2021). The high abundance of these two components strongly suggests a highly branched or “hairy” structure, which is crucial for the functional properties of RG-I.

The core backbone of the rhamnogalacturonan structure was quantified through its constituent parts: RhaOS were present at 7.0 ± 0.6%, and OGalA, representing the homogalacturonan “smooth” regions, were found at 6.4 ± 0.6%. Furthermore, a notable presence of GlcOS was detected at 19.9 ± 1.6%. In summary, these compositional parameters reveal a complex pectin dominated by highly branched RG-I domains, underscoring its potential for applications where such structural features are advantageous.

3.6. Production of 2,3-Butanediol from enzymatic hydrolysates of pretreated AP residue

3.6.1. Characterization pretreated AP

As a result of AP pretreatment under optimal conditions, a solid residue (pretreated AP) was obtained with a markedly reconfigured composition (see Supplementary Material, Table S1). Galacturonan and rhamnan were completely extracted (0.0 ± 0.0%), while arabinan decreased to 0.2 ± 0.1% and galactan to 10.0 ± 0.4%. In contrast, glucan concentration increased from 28.7% to 37.1%, representing a 29.3% relative enrichment of the cellulose fraction in the pretreated solid residue compared to the raw AP. Consistent with microwave-pretreated pectin-rich biomass (Costa et al., 2025), lignin was redistributed between acid-insoluble (decreased 3.4 ± 0.0%) and acid-soluble (increased 23.5 ± 0.5%) fractions, accompanied by minor ash reduction (0.4 ± 0.1%) and the complete removal of extractives.

On a compositional basis, the pretreated AP contained 37.1 g glucan and 10.0 g arabinan per 100 g solid, corresponding to retentions of 66.3% and 46.9% of their original amounts in raw AP (see Supplementary Material, Table S1). The pretreatment efficiently solubilizes pectin and enriches glucan, yielding a solid residue optimized for sequential enzymatic hydrolysis and 2,3-BDO fermentation.

3.6.2. Enzimatic hydrolysis and fermentation

In the first step of enzymatic hydrolysis, two different substrate loadings (10 and 15% *w/v*) were studied, two enzymatic hydrolysates being obtained with a total sugars content of 43.8 g/L (glucose, 34.7 g/L; galactose, 7.9 g/L; and arabinose, 1.2 g/L) and 59.2 g/L (glucose, 48.0 g/L; galactose, 9.9 g/L; and arabinose, 1.4 g/L), respectively. Thus, high total sugars recoveries (g total sugars by enzymatic hydrolysis/100 g total sugars in pretreated AP) were obtained: 75.5 and 83.7% for 10 and 15% w/v substrate loadings, respectively.

Subsequently, in the second step of 2,3-BDO fermentation, both the 10 and 15% (*w/v*) enzymatic hydrolysates obtained were submitted to a 2,3-BDO fermentation process, using two different 2,3-BDO-producing strains (*B. licheniformis* and *B. amyloliquefaciens*). The results obtained are shown in Fig. 3 and Table 3.

Regarding 2,3-BDO fermentation by *B. licheniformis,* as can be appreciated in Fig. 3A, all sugars were completely consumed in only 48 h of process for both 10 and 15% (w/v) enzymatic hydrolysates, sugar uptakes of about 80% being already reached at fermentation times as short as 22 h of process. However, glucose was consumed much more quickly than galactose and arabinose (in only 24 h of process vs 48 h), with consumption rates of 1.46–2.10 g glucose/L·h vs 0.17–0.24 g galactose/L·h and 0.04–0.05 g arabinose/L·h (data not shown). The hierarchical utilization of sugars observed in this study—where glucose is rapidly exhausted before the substantial metabolism of galactose and arabinose—is a classic manifestation of carbon catabolite repression (CCR) (Tinôco et al., 2021b). In *Bacillus* species, this global regulatory mechanism is primarily mediated by the transcription factor CcpA (Catabolite Control Protein A) and its co-effector, the seryl-phosphorylated form of the phosphocarrier protein HPr (P-Ser-HPr). During rapid glucose consumption, the high glycolytic flux results in a significant increase in the intracellular concentration of fructose−1,6-bisphosphate (FBP). In this context, FBP serves as a precise metabolic sensor and allosteric activator of the bifunctional enzyme HPr kinase/phosphatase (HprK). Specifically, FBP binds to HprK, markedly stimulating its kinase activity while simultaneously inhibiting its opposing phosphatase activity. This allosteric shift ensures the rapid ATP-dependent phosphorylation of HPr at the Ser46 residue, facilitating the formation of the CcpA/P-Ser-HPr complex. This complex subsequently binds to highly conserved *cis*-acting sequences known as catabolite-responsive elements (*cre* sites) located within or adjacent the promoter regions of alternative sugar operons, such as the *gal* (galactose) and *ara* (arabinose) clusters. This binding event transcriptionally represses the genes encoding the transporters and catabolic enzymes required for alternative sugar metabolism, thereby ensuring the preferential utilization of the most energetically favorable substrate.

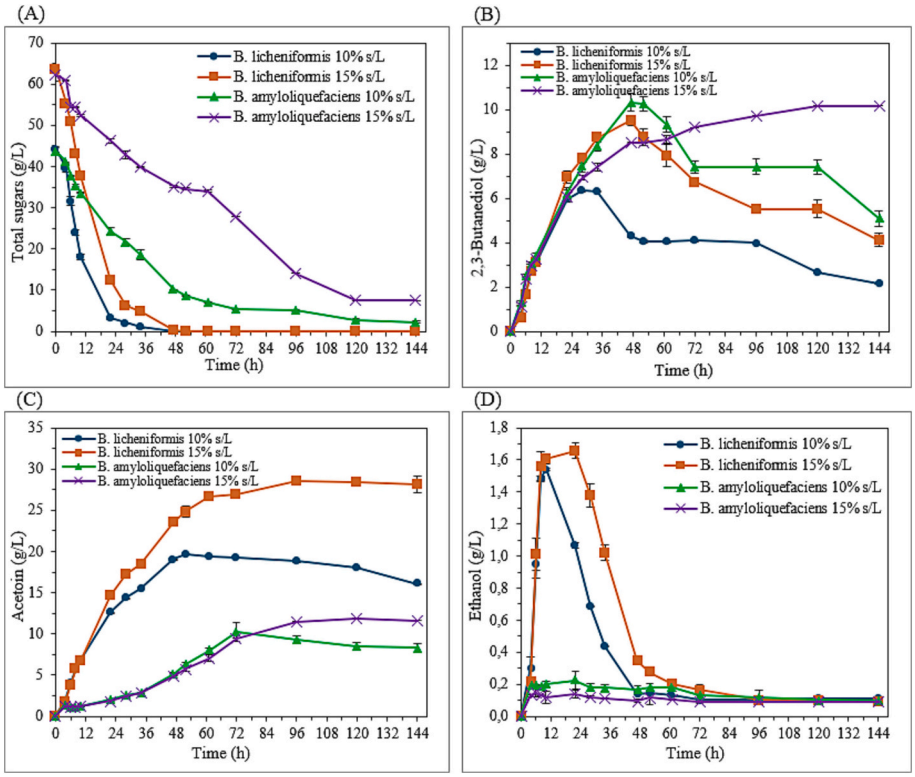

Fig. 3. 2,3-butanediol fermentation kinetics of pretreated apple residue enzymatic hydrolysates (at 10 and 15% (*w/v*) of substrate loading) by *B. licheniformis* and *B. amyloliquefaciens*. Total sugars consumption (A), and 2,3-butanediol (B), acetoin (C) and ethanol (D) production.

Table 3
2,3-butanediol fermentation of pretreated apple residue enzymatic hydrolysates (at 10 and 15% (w/v) of substrate loading) by *B. licheniformis* and *B. amyloliquefaciens*. Sugar uptake (%); 2,3-butanediol (2,3-BDO), ethanol, and acetoin concentrations (g/L); biomass OD (600 nm); and butanediol yield ($Y_{BDO/sugars}$, expressed as g/g sugars consumed) and productivity (Q_{BDO}, expressed as g/L·h) at the time of maximum butanediol production. Data in parentheses refers to sugar uptake at the end of the fermentation process (144 h).

Microorganism	Solids loading (%, w/v)	Time (h)	Sugar uptake (%)	2,3-BDO (g/L)	Ethanol (g/L)	Acetoin (g/L)	Biomass OD (600 nm)	$Y_{BDO/sugars}$ (g/g)	Q_{BDO} (g/L·h)
B. licheniformis	10	28	95.4 (100)	6.3 ± 0.0*	0.7 ± 0.0	14.4 ± 0.0*	12.6 ± 0.0	0.15	0.227
	15	47	100 (100)	9.5 ± 0.2*	0.4 ± 0.0	23.6 ± 0.4*	15.5 ± 0.3	0.15	0.202
B. amyloliquefaciens	10	47	76.7 (94.7)	10.3 ± 0.4	0.2 ± 0.0	5.1 ± 0.2*	9.7 ± 0.2	0.31	0.220*
	15	120	88.0 (88.0)	10.2 ± 0.0	0.1 ± 0.0	11.9 ± 0.0*	13.7 ± 0.1	0.19	0.085*

Statistical differences between substrate loadings (10 vs 15%) and between *B. licheniformis* and *B. amyloliquefaciens* at the same substrate loading were evaluated using Student's t-test. * indicates statistically significant differences ($p < 0.05$).

Consequently, the consumption rates for galactose and arabinose remained significantly lower (0.04–0.24 g/L·h) until glucose depletion at approximately 24 h relieved this repression (Deutscher, 2008; Ma et al., 2018). Such sequential uptake is a strategic metabolic response in *Bacillus* strains to optimize energetic efficiency and maintain redox balance during the production of metabolites like 2,3-BDO (Song et al., 2019).

On the other hand, as is shown in Fig. 3B and Table 3, when substrate loading increased from 10 to 15%, the maximum 2,3-BDO levels attained increased significantly ($p < 0.05$) from 6.3 to 9.5 g/L (increase of 50.8%). 2,3-BDO yields and productivities reached at the time of maximum 2,3-BDO production ($t = 28$ and 47 h for 10 and 15% enzymatic hydrolysates, respectively) were of 0.15 g/g and 0.202–0.227 g/L·h, respectively (Table 3). Then, in this case, the increase in substrate loading from 10 to 15% did not negatively influence the 2,3-BDO yield and productivity achieved by *B. licheniformis*, which could be very interesting for the economic profitability of the process.

Concerning 2,3-BDO fermentation by *B. amyloliquefaciens,* high total sugar consumptions (>88%) were determined at the end of fermentation ($t = 144$ h) (Fig. 3A and Table 3), only glucose being completely metabolized (data not shown). In this case, similar maximum 2,3-BDO concentrations (about 10 g/L) were analysed for both solid loadings (Fig. 3B and Table 3). However, as can be seen in Table 3, butanol yields (0.19 vs 0.31 g/g) and productivities (0.085 vs 0.220 g/L·h) were much lower when solid loading was increased from 10 to 15% (*w/v*).

2,3-BDO is not the only fermentation product originated by *Bacillus* strains, but other by-products are also detected, for instance acetoin (Fig. 3C) and ethanol (Fig. 3D). Acetoin is generated by successive α-acetolactate synthase and 4,α-acetolactate decarboxylase pathways; while ethanol is generated through successive pyruvate–formate lyase, acetaldehyde dehydrogenase, and ethanol dehydrogenase pathways (Hakizimana et al., 2020). Although ethanol levels observed are low (0.1–0.7 g/L) (Table 3 and Fig. 3D), high acetoin concentrations (5.1–23.6 g/L) can be obtained at the time of maximum 2,3-BDO production (Table 3 and Fig. 3C), especially by *B. licheniformis*. In this way, under the evaluated conditions, acetoin was identified as the primary fermentation product, with concentrations significantly exceeding those of 2,3-BDO (5.1–23.6 g/L vs 6.3–10.3 g/L), particularly in *B. licheniformis* cultures. This metabolic profile is characteristic of many *Bacillus* strains, which utilize the acetoin/2,3-BDO pathway to prevent intracellular acidification and regulate the.

NADH/NAD^+ ratio (Maina et al., 2022). The substantial accumulation of acetoin (up to 23.6 g/L), particularly in *B. licheniformis* cultures, is indicative of the limitations inherent to shake-flask fermentations, where the lack of active pH control and fixed oxygen transfer rates (OTR) shift the intracellular redox state toward an oxidative profile. The reversible conversion between acetoin and 2,3-BDO is governed by the intracellular redox state and the NADH/NAD^+ ratio. Under conditions of relatively high oxygen availability, NADH is preferentially utilized for aerobic respiration, limiting its availability for the 2,3-butanediol dehydrogenase (BDH)-mediated reduction of acetoin. Consequently, 2,3-BDO production is maximized under microaerophilic conditions, where oxygen limitation triggers the reduction of acetoin to 2,3-BDO as a mechanism to regenerate NAD^+ and maintain glycolytic flux (Tinôco et al., 2021c). It is important to note that while 2,3-BDO is the target metabolite, acetoin is a highly versatile platform chemical with extensive industrial applications as a flavor agent and chemical precursor (Maina et al., 2022). The simultaneous production of these two four-carbon compounds underscores the potential of the pretreated AP hydrolysates to serve as a feedstock for a dual-product biorefinery. Nevertheless, as discussed previously, shifting the metabolic equilibrium toward 2,3-BDO is feasible through the implementation of more stringent microaerophilic conditions (e.g., reduced agitation, increased working volumes and/or the need for instrumented systems) to favor the reductive step of the pathway.

In addition, as can be observed in Fig. 3A and B, the 2,3-BDO generated was also metabolized when low sugar concentrations were detected in the fermentation broth. According to Maina et al. (2022), 2,3-BDO can be reversibly turned into acetoin, regenerating the NADH, with a continuous oxidation–reduction state. This behavior was not observed in the fermentation of 15% enzymatic hydrolysate by *B. amyloliquefaciens* (Fig. 3B), since in this case the sugar levels were quite considerable during the whole fermentation (except during the last hours of the process ($t > 120$ h)) (Fig. 3A). In this case, the higher substrate loading (15% w/v) likely exerted a dual effect on the fermentation environment, favoring the metabolic shift toward 2,3-BDO. First, the increased concentration of hydrolysate elevates the medium's viscosity, which reduces the OTR. Simultaneously, the higher availability of fermentable sugars supports increased metabolic activity and biomass growth, significantly raising the oxygen uptake rate (OUR). When the OUR exceeds the OTR, the dissolved oxygen levels decline rapidly, establishing a microaerophilic environment (Hakizimana et al., 2020; Tinôco et al., 2021c). Under such oxygen-limited conditions, *Bacillus* species activate the 2,3-BDO pathway as a biological “redox sink” to regenerate NAD^+ from NADH, thereby maintaining the intracellular redox balance required for continued glycolysis (Maina et al., 2022; Song et al., 2019). This phenomenon, coupled with the extended fermentation time, ensured a prolonged period of oxygen limitation, which is a critical prerequisite for driving the reduction of acetoin into 2,3-BDO rather than allowing its accumulation as an oxidized byproduct.

A comparative assessment of the two strains revealed distinct metabolic strategies governed by substrate loading and oxygen availability. At the lower substrate loading (10%), *B. amyloliquefaciens* demonstrated superior metabolic efficiency, yielding significantly higher 2,3-BDO concentrations (10.3 vs 6.3 g/L) and yields (0.31 vs 0.15 g/g) compared to *B. licheniformis* (Table 3 and Fig. 3B). This performance at lower sugar concentrations suggests a tightly regulated metabolic flux where pyruvate is efficiently channeled toward the α-acetolactate pathway with minimal diversion to organic acids or ethanol (Hakizimana et al., 2020). This was accompanied by minimal by-product formation (at the time of 2,3-BDO production maximum), as ethanol and acetoin levels remained markedly lower than those observed for *B. licheniformis* (0.2 vs 0.7 g/L and 5.1 vs 14.4 g/L,

respectively) (Table 3 and Fig. 3C, D). However, a profound metabolic shift occurred at the 15% (*w/v*) loading. While *B. amyloliquefaciens* maintained its 2,3-BDO levels (9.5–10.2 g/L), its fermentation kinetics were severely protracted, requiring 120 h for completion. This suggests a sensitivity to substrate inhibition or osmotic stress induced by high initial sugar concentrations, which can impair membrane transport and glycolytic enzyme activity (Celińska and Grajek, 2009). In stark contrast, *B. licheniformis* demonstrated remarkable metabolic robustness under high-solid conditions, reaching maximum production in only 47 h (Fig. 3)—a 2.4-fold increase in productivity (0.202 vs. 0.085 g/L·h) compared to its counterpart (Table 3). The robustness of *B. licheniformis* at higher sugar concentrations is further highlighted by its ability to simultaneously produce high titers of both 2,3-BDO and acetoin (up to 23.6 g/L at the time of 2,3-BDO production maximum) from the onset of fermentation (Fig. 3B and C) (Guragain et al., 2017; López-Linares et al., 2025a), which is indicative of overflow metabolism. High glycolytic flux, driven by rapid glucose uptake, likely saturated the TCA cycle, necessitating the activation of the acetoin/2,3-BDO pathway as an alternative route to prevent the accumulation of toxic pyruvate and to maintain the intracellular pH (Celińska and Grajek, 2009; Maina et al., 2022). The significant acetoin accumulation (23.6 g/L) in *B. licheniformis* further suggests that its 2,3-butanediol dehydrogenase (BDH) activity may be more sensitive to the NAD+/NADH ratio than that of *B. amyloliquefaciens*. In contrast, *B. amyloliquefaciens* showed a stagnant acetoin production phase during the initial stages, with accumulation occurring only as sugar levels reached depletion. These observations align with previous studies suggesting that while *B. amyloliquefaciens* is more efficient under carbon-limited conditions (López-Linares et al., 2025a; Yang et al., 2015), *B. licheniformis* possesses the metabolic vigor required for high-solid loadings, where rapid substrate turnover and high volumetric productivity are paramount for industrial viability (Guragain et al., 2017; López-Linares et al., 2025a). This same behavior was also reported by López-Linares et al. (2025a) in 2,3-BDO fermentation assays by *B. licheniformis* DSM 8785 and *B. amyloliquefaciens* DSM 7 with glucose semi-defined media (20 to 120 g/L), using also shake flasks and under the same experimental conditions used in this study.

Therefore, in brief, the use of *B. amyloliquefaciens* could be advisable for 2,3-BDO production at lower substrate loadings (10%), while *B. licheniformis* could be better for 2,3-BDO fermentations at higher substrate loadings (15%). Comparing the best results achieved in this work (10.3 g/L 2,3-BDO, 4.3 g 2,3-BDO/100 g AP, 0.31 g/g and 0.220 g/L·h) with those reported in the literature, comparable or lower 2,3-BDO concentrations have been obtained from a variety of agro-industrial residues using different microbial systems. Not very different 2,3-BDO levels (12.8 g/L) from those obtained in this work were determined by Białkowska et al. (2016) from apple pomace enzymatic hydrolysate, also using a *Bacillus* strain (*B. subtilis* LOCK 1086). Much lower 2,3-BDO concentration (3.7 g/L), yield (0.14 g/g) and productivity (0.10 g/L·h) than those attained in this work were obtained in the *co*-culture fermentation by *Paenibacillus polymyxa* DSM 365; while *Rhodococcus* sp. of brewer's spent grain hemicellulosic hydrolysate (López-Linares et al., 2025b; Yang et al., 2015) reported similar 2,3-BDO yields (0.29–0.30 g/g) to those obtained in this work in the direct fermentation of spirit-based distillers' grain (SDG) by *B. amyloliquefaciens* B10–127. 16.5, 10.7; while 5 g/L 2,3-BDO were also determined from enzymatic hydrolysates of apple pomace, dried sugar beet pulp, and potato pulp, respectively, by *B. amyloliquefaciens* TUL 308 (Białkowska et al., 2015; Sikora et al., 2016) reported similar 2,3-BDO concentration (11.6 g/L) to those obtained in this work, in 2,3-BDO fermentation by *B. licheniformis* NCIMB 8059, and also using enzymatic apple pomace hydrolysate.

3.7. Process scalability and techno-economic outlook

The proposed biorefinery demonstrates significant industrial potential by co-producing POS and 2,3-BDO through a water-only, energy-efficient MAE process. This approach minimizes operational expenditures (OPEX) and environmental impact by eliminating hazardous organic solvents and reducing thermal energy requirements. However, to optimize downstream economics, future scale-up efforts must transition from empirical observations to similarity-based design criteria. For the MAE stage, the Specific Energy Input (SEI), defined as the ratio of microwave power to total slurry mass (J/g), must remain constant to ensure reproducible pectin yields. Based on the optimized conditions (600 W, 8.1 min, 10% solids loading), a SEI of approximately 5.3 kJ/g was applied in this study. Given the limited penetration depth of microwaves, a modular scale-up approach or a continuous-flow system with a constant surface-to-volume ratio is recommended to maintain thermal homogeneity. Regarding the UF unit, the scaling law follows the Resistance-in-Series model, where the membrane area is determined by the target processing time and the flux decline kinetics ($K_c = 3{\cdot}10^7$ s/m^2) observed in this study. To minimize fouling, the crossflow velocity must be adjusted to maintain a constant shear rate at the wall, preventing the accumulation of high-molecular-weight RG-I fragments.

Finally, for the fermentation stage, the matching relationship between aeration (vvm) and stirring speed (N) must be governed by a constant $k_L{\cdot}a$ a strategy. Based on the metabolic robustness of *B. licheniformis* observed at 15% solids loading, a $k_L{\cdot}a$ a value between 15 and 30 h^{-1} is proposed as the scaling criterion to maintain the microaerophilic conditions necessary for the biological 'redox sink' to favor 2,3-BDO accumulation over acetoin. Crucially, the move to instrumented stirred-tank bioreactors (STRs) will address current limitations by allowing for the automated, real-time control of pH and OTR, thereby maximizing the reductive metabolic flux toward 2,3-BDO. Overall, the integration of these similarity-based criteria provides a realistic roadmap for process intensification, bridging the gap between laboratory-scale screening and industrial-scale production while enhancing the practical operability of the apple pomace biorefinery.

4. Conclusions

This study validates an integrated, solvent-free biorefinery for apple pomace for the co-production of POS and 2,3-BDO, confirming the scientific and technical feasibility of a modular MAE → UF → SHF configuration. The primary scientific contribution lies in demonstrating that ultrafiltration (3 kDa) serves as a superior alternative to conventional ethanol precipitation, effectively concentrating POS to 47.5 ± 0.1 g/L while retaining bioactive neutral fractions typically lost in solvent-based methods. Under optimized MAE conditions (136 °C, 8.1 min), a pectin yield of 22.3 ± 0.2% (g pectin/100 g dry AP) was secured alongside an overall POS recovery of 61.5%. Simultaneously, the process enabled the complete valorization of the solid residue (enriched to 37% glucan) into 2,3-BDO, achieving concentrations up to 10.3 g/L via *Bacillus* fermentation. These results establish a scalable, water-only route that maximizes feedstock utility, aligning fruit processing by-products with circular bioeconomy goals.

CRediT authorship contribution statement

Alberto Lozano: Writing – original draft, Investigation, Data curation. **Alba Mei González-Galán:** Writing – original draft, Investigation, Data curation. **Juan Carlos López-Linares:** Writing – original draft, Methodology, Investigation. **Mónica Coca:** Supervision, Methodology, Conceptualization. **María Teresa García-Cubero:** Supervision, Funding acquisition, Conceptualization. **Susana Lucas:** Writing – review & editing, Supervision, Methodology, Conceptualization.

Declaration of competing interest

The authors declare that they have no known competing financial interests or personal relationships that could have appeared to influence the work reported in this paper.

Acknowledgments

The authors acknowledge the financial support from the Ministry of Science, Innovation and Universities, the Spanish State Research Agency and the European Regional Development Fund (project PID2023-147967OB-I00/MCIU/AEI /10.13039/501100011033/ERDF, EU), as well as from the Department of Education of the Regional Government of Castilla y León, co-financed by the European Union through the European Regional Development Fund (ERDF) (CLU-2025-2-06, UIC 320). The authors also wish to thank Muns Agroindustrial (Lérida, Spain) for kindly providing the apple pomace used in this study.

Appendix A. Supplementary data

Supplementary data to this article can be found online at https://doi.org/10.1016/j.biteb.2026.102638.

Data availability

Data will be made available on request.

References

Antov, M.G., Perović, M.N., Milošević, M.M., 2023. Integration of enzymatic modification and ultrafiltration for the production of pectin fractions with highly potent antioxidant capacity as green valorization of sugar beet pulp. Bioprocess Biosyst. Eng. 46, 157–164. https://doi.org/10.1007/S00449-022-02830-9/TABLES/2.

Batista, G., Souza, R.B.A., Pratto, B., dos Santos-Rocha, M.S.R., Cruz, A.J.G., 2019. Effect of severity factor on the hydrothermal pretreatment of sugarcane straw. Bioresour. Technol. 275, 321–327. https://doi.org/10.1016/J.BIORTECH.2018.12.073.

Białkowska, A.M., Gromek, E., Krysiak, J., Sikora, B., Kalinowska, H., Jędrzejczak-Krzepkowska, M., Kubik, C., Lang, S., Schütt, F., Turkiewicz, M., 2015. Application of enzymatic apple pomace hydrolysate to production of 2,3-butanediol by alkaliphilic *Bacillus licheniformis* NCIMB 8059. J. Ind. Microbiol. Biotechnol. 42, 1609–1621. https://doi.org/10.1007/S10295-015-1697-3.

Białkowska, A.M., Jędrzejczak-Krzepkowska, M., Gromek, E., Krysiak, J., Sikora, B., Kalinowska, H., Kubik, C., Schütt, F., Turkiewicz, M., 2016. Effects of genetic modifications and fermentation conditions on 2,3-butanediol production by alkaliphilic *Bacillus subtilis*. Appl. Microbiol. Biotechnol. 100, 2663–2676. https://doi.org/10.1007/S00253-015-7164-2.

Bravo-Venegas, J., Prado-Acebo, I., Gullón, B., Lú-Chau, T.A., Eibes, G., 2023. Avoiding acid crash: from apple pomace hydrolysate to butanol through acetone-butanol-ethanol fermentation in a zero-waste approach. Waste Manag. 164, 47–56. https://doi.org/10.1016/j.wasman.2023.03.039.

Cais-Sokolińska, D., Kaczyński, Ł.K., Bielska, P., 2022. Inhibition of galactooligosaccharide (GOS) degradation in high-heat-treated goat's milk as a raw material for functional dairy products. Appl. Sci. 12, 11639. https://doi.org/10.3390/APP122211639.

Celińska, E., Grajek, W., 2009. Biotechnological production of 2,3-butanediol-current state and prospects. Biotechnol. Adv. 27, 715–725. https://doi.org/10.1016/j.biotechadv.2009.05.002.

Chen, M., Lahaye, M., 2021. Natural deep eutectic solvents pretreatment as an aid for pectin extraction from apple pomace. Food Hydrocoll. 115, 106601. https://doi.org/10.1016/J.FOODHYD.2021.106601.

Costa, J.M., Wang, W., Nakasu, P.Y.S., Hu, C., Forster-Carneiro, T., Hallett, J.P., 2025. Impacts of microwaves on the pectin extraction from apple pomace: Technological properties in structuring of hydrogels. Food Hydrocoll. 160, 110766. https://doi.org/10.1016/J.FOODHYD.2024.110766.

del Amo-Mateos, E., Cáceres, B., Coca, M., Teresa García-Cubero, M., Lucas, S., 2024. Recovering rhamnogalacturonan-I pectin from sugar beet pulp using a sequential ultrasound and microwave-assisted extraction: study on extraction optimization and membrane purification. Bioresour. Technol. 394, 130263. https://doi.org/10.1016/J.BIORTECH.2023.130263.

Deutscher, J., 2008. The mechanisms of carbon catabolite repression in bacteria. Curr. Opin. Microbiol. 11, 87–93. https://doi.org/10.1016/j.mib.2008.02.007.

Fariñas-Mera, R., Celeiro, M., Prado-Acebo, I., Lu-Chau, T.A., García-Jares, C., Eibes, G., 2025. Apple pomace valorisation into antioxidant polyphenols: multi-criteria process design. Ind. Crop. Prod. 231. https://doi.org/10.1016/j.indcrop.2025.121203.

Gawal, P.M., Lataye, S., 2025. Enhanced 2,3-butanediol recovery from fermentation broth: a study on isobutanol/sodium chloride aqueous two-phase systems. Biotechnol. Bioprocess Eng. 30 (3), 562–572. https://doi.org/10.1007/S12257-025-00186-X.

Gawal, P.M., Subudhi, S., 2023. Advances and challenges in bio-based 2,3-BD downstream purification: a comprehensive review. Bioresour. Technol. Rep. 24, 101638. https://doi.org/10.1016/J.BITEB.2023.101638.

Girón-Hernández, J., Pazmino, M., Barrios-Rodríguez, Y.F., Turo, C.T., Wills, C., Cucinotta, F., Benlloch-Tinoco, M., Gentile, P., 2023. Exploring the effect of utilising organic acid solutions in ultrasound-assisted extraction of pectin from apple pomace, and its potential for biomedical purposes. Heliyon 9, e17736. https://doi.org/10.1016/J.HELIYON.2023.E17736.

Guo, R., Fan, R., Hu, J., Zhang, X., Han, L., Wang, M., He, C., 2024. Valorization of apple pomace: Structural and rheological characterization of low-Methoxyl Pectins extracted with green agents of citric acid/sodium citrate. Food Chem. X 24, 102010. https://doi.org/10.1016/J.FOCHX.2024.102010.

Guragain, Y.N., Chitta, D., Karanjikar, M., Vadlani, P.V., 2017. Appropriate lignocellulosic biomass processing strategies for efficient 2,3-butanediol production from biomass-derived sugars using *Bacillus licheniformis* DSM 8785. Food Bioprod. Process. 104, 147–158. https://doi.org/10.1016/J.FBP.2017.05.010.

Hakizimana, O., Matabaro, E., Lee, B.H., 2020. The current strategies and parameters for the enhanced microbial production of 2,3-butanediol. Biotechnol. Reports 25, e00397. https://doi.org/10.1016/J.BTRE.2019.E00397.

Huang, Y.P., Robinson, R.C., Barile, D., 2022. Food glycomics: dealing with unexpected degradation of oligosaccharides during sample preparation and analysis. J. Food Drug Anal. 30, 62. https://doi.org/10.38212/2224-6614.3393.

Jasińska, K., Nowosad, M., Perzyna, A., Bielacki, A., Dziwiński, S., Zieniuk, B., Fabiszewska, A., 2024. Sustainable lipase immobilization: chokeberry and apple waste as carriers. Biomolecules 14. https://doi.org/10.3390/BIOM14121564.

Jia, Y., Wang, C., Khalifa, I., Zhu, Y., Wang, Z., Chen, H., Liang, X., Zhang, H., Hu, L., Yang, W., 2024. Pectin: a review with recent advances in the emerging revolution and multiscale evaluation approaches of its emulsifying characteristics. Food Hydrocoll. 157, 110428. https://doi.org/10.1016/J.FOODHYD.2024.110428.

Jurchescu, I.M., Hamann, J., Zhou, X., Ortmann, T., Kuenz, A., Prüße, U., Lang, S., 2013. Enhanced 2,3-butanediol production in fed-batch cultures of free and immobilized *Bacillus licheniformis* DSM 8785. Appl. Microbiol. Biotechnol. 97, 6715–6723. https://doi.org/10.1007/S00253-013-4981-Z.

Kauser, S., Murtaza, M.A., Hussain, A., Imran, M., Kabir, K., Najam, A., An, Q.U., Akram, S., Fatima, H., Batool, S.A., Shehzad, A., Yaqub, S., 2024. Apple pomace, a bioresource of functional and nutritional components with potential of utilization in different food formulations: a review. Food Chem. Adv. 4, 100598. https://doi.org/10.1016/J.FOCHA.2023.100598.

Lim, A.L., Bai, R., 2003. Membrane fouling and cleaning in microfiltration of activated sludge wastewater. J. Membr. Sci. 216, 279–290. https://doi.org/10.1016/S0376-7388(03)00083-8.

López-Linares, Juan C., Rama, E., García-Cubero, M.T., Coca, M., Perez, C.L., Yamakawa, C.K., Dragone, G., Mussatto, S.I., 2025b. Enhancing 2,3-butanediol and acetoin production from brewer's spent grain hemicellulosic hydrolysate through bacterial co-cultivation. New Biotechnol. 88, 22–31. https://doi.org/10.1016/J.NBT.2025.03.006.

López-Linares, Juan Carlos, González-Galán, A.M., Coca, M., Lucas, S., García-Cubero, M. T., 2025a. Harnessing carrot discard as a novel feedstock for 2,3-butanediol bioproduction: a comparison of fermentation strategies and *Bacillus* performance. Appl. Sci. (Switz.) 15, 7808. https://doi.org/10.3390/APP15147808/S1.

Ma, K., He, M., You, H., Pan, L., Wang, Z., Wang, Y., Hu, G., Cui, Y., Maeda, T., 2018. Improvement of (R,R)-2,3-butanediol production from corn stover hydrolysate by cell recycling continuous fermentation. Chem. Eng. J. 332, 361–369. https://doi.org/10.1016/J.CEJ.2017.09.097.

Ma, X., Ma, Y., Zhang, L., Zhao, Y., Lei, J., Wang, Y., Liu, M., Lü, X., Wang, X., 2024. Subcritical water pretreatment of de-pectin apple pomace for ethanol conversion and whole components utilization. Ind. Crop. Prod. 216. https://doi.org/10.1016/j.indcrop.2024.118720.

MacAskill, J.J., Suckling, I.D., Lloyd, J.A., Manley-Harris, M., 2018. Unravelling the effect of pretreatment severity on the balance of cellulose accessibility and substrate composition on enzymatic digestibility of steam-pretreated softwood. Biomass Bioenergy 109, 284–290. https://doi.org/10.1016/J.BIOMBIOE.2017.12.018.

Maina, S., Prabhu, A.A., Vivek, N., Vlysidis, A., Koutinas, A., Kumar, V., 2022. Prospects on bio-based 2,3-butanediol and acetoin production: recent progress and advances. Biotechnol. Adv. 54. https://doi.org/10.1016/j.biotechadv.2021.107783.

Matharu, A.S., Houghton, J.A., Lucas-Torres, C., Moreno, A., 2016. Acid-free microwave-assisted hydrothermal extraction of pectin and porous cellulose from mango peel waste – towards a zero waste mango biorefinery. Green Chem. 18, 5280–5287. https://doi.org/10.1039/C6GC01178K.

Orrego, D., Olivares-Tenorio, M.L., Hoyos, L.V., Alvarez-Vasco, C., Klotz-Ceberio, B., Caicedo, N., 2024. Towards a sustainable circular bioprocess: pectic oligosaccharides (POS) enzymatic production using passion fruit peels. LWT 207. https://doi.org/10.1016/J.LWT.2024.116681.

Roman-Benn, A., Contador, C.A., Li, M.W., Lam, H.M., Ah-Hen, K., Ulloa, P.E., Ravanal, M.C., 2023. Pectin: An overview of sources, extraction and applications in food products, biomedical, pharmaceutical and environmental issues. Food Chem. Adv. 2, 100192. https://doi.org/10.1016/J.FOCHA.2023.100192.

Ruiz, M.O., Benito-Román, Beltrán, S., Sanz, M.T., 2024. Fractionation and refining of pectic oligosaccharides derived from onion skins through continuous feed diafiltration. J. Membr. Sci. 708. https://doi.org/10.1016/j.memsci.2024.123054.

Sikora, B., Kubik, C., Kalinowska, H., Gromek, E., Białkowska, A., Jędrzejczak-Krzepkowska, M., Schüett, F., Turkiewicz, M., 2016. Application of byproducts from food processing for production of 2,3-butanediol using *Bacillus amyloliquefaciens* TUL 308. Prep. Biochem. Biotechnol. 46, 610–619. https://doi.org/10.1080/10826068.2015.1085401.

Sluiter, A., Hames, B., Ruiz, R., Scarlata, C., Sluiter, J., Templeton, D., 2008a. Determination of Ash in Biomass: Laboratory Analytical Procedure (LAP); Issue Date: 7/17/2005.

Sluiter, A., Hames, B., Ruiz, R., Scarlata, C., Sluiter, J., Templeton, D., Crocker, D., 2008b. Determination of Structural Carbohydrates and Lignin in Biomass: Laboratory Analytical Procedure (LAP) (Revised July 2011).

Sluiter, A., Ruiz, R., Scarlata, C., Sluiter, J., Templeton, D., 2008c. Determination of Extractives in Biomass: Laboratory Analytical Procedure (LAP); Issue Date 7/17/2005.

Song, C.W., Park, J.M., Chung, S.C., Lee, S.Y., Song, H., 2019. Microbial production of 2,3-butanediol for industrial applications. J. Ind. Microbiol. Biotechnol. 46, 1583–1601. https://doi.org/10.1007/S10295-019-02231-0.

Spinei, M., Oroian, M., 2022. Microwave-assisted extraction of pectin from grape pomace. Sci. Rep. 12 (1), 12722. https://doi.org/10.1038/s41598-022-16858-0.

Tinôco, D., Borschiver, S., Coutinho, P.L., Freire, D.M.G., 2021a. Technological development of the bio-based 2,3-butanediol process. Biofuels Bioprod. Biorefin. 15, 357–376. https://doi.org/10.1002/BBB.2173.

Tinôco, D., de Castro, A.M., Seldin, L., Freire, D.M.G., 2021b. Production of (2R,3R)-butanediol by *Paenibacillus polymyxa* PM 3605 from crude glycerol supplemented with sugarcane molasses. Process Biochem. 106, 88–95. https://doi.org/10.1016/J.PROCBIO.2021.03.030.

Tinôco, D., Pateraki, C., Koutinas, A.A., Freire, D.M.G., 2021c. Bioprocess Development for 2,3-Butanediol Production by *Paenibacillus* Strains. ChemBioEng Reviews 8, 44–62. https://doi.org/10.1002/CBEN.202000022.

Tsirigotis-Maniecka, M., Górska, E., Mazurek-Hołys, A., Pawlaczyk-Graja, I., 2024. Unlocking the potential of food waste: a review of multifunctional pectins. Polymers 16, 2670. https://doi.org/10.3390/POLYM16182670.

Viegas, À., Alegria, M.J., Raymundo, A., 2024. Sustainable jam with apple pomace: gelling, rheology, and composition analysis. Gels. https://doi.org/10.3390/gels10090580.

Wang, R., Xu, Z., Jiang, D., Xiong, X., Li, Y., Li, X., 2025. Optimization of ohmic heating extraction of pectin from apple pomace and comparison with conventional method. Food Bioprod. Process. 151, 231–241. https://doi.org/10.1016/j.fbp.2025.03.010.

Yang, T., Rao, Z., Zhang, X., Xu, M., Xu, Z., Yang, S.T., 2015. Economic conversion of spirit-based distillers' grain to 2,3-butanediol by *Bacillus amyloliquefaciens*. Process Biochem. 50, 20–23. https://doi.org/10.1016/J.PROCBIO.2014.11.006.

Yilmaz-Turan, S., Gál, T., Lopez-Sanchez, P., Martinez, M.M., Menzel, C., Vilaplana, F., 2023. Modulating temperature and pH during subcritical water extraction tunes the molecular properties of apple pomace pectin as food gels and emulsifiers. Food Hydrocoll. 145, 109148. https://doi.org/10.1016/J.FOODHYD.2023.109148.

Zheng, J., Li, H., Wang, D., Li, R., Wang, S., Ling, B., 2021. Radio frequency assisted extraction of pectin from apple pomace: Process optimization and comparison with microwave and conventional methods. Food Hydrocoll. 121, 107031. https://doi.org/10.1016/J.FOODHYD.2021.107031.

Ziadi, M., Bouzaiene, T., M'Hir, S., Zaafouri, K., Mokhtar, F., Hamdi, M., Boisset-Helbert, C., 2018. Evaluation of the efficiency of ethanol precipitation and ultrafiltration on the purification and characteristics of exopolysaccharides produced by three lactic acid bacteria. Biomed. Res. Int. 2018. https://doi.org/10.1155/2018/1896240.